**Advances in Concrete Construction**, *Vol. 9, No. 4 (2020) 423-435*
DOI: https://doi.org/10.12989/acc.2020.9.4.423


# Evaluation of seismic strengthening techniques for non-ductile soft-story RC frame

Prajwol Karki[1a], Romanbabu M. Oinam[2b] and Dipti Ranjan Sahoo[*1]

*[1]Department of Civil Engineering, Indian Institute of Technology Delhi, New Delhi-110016, India*
*[2]Department of Civil & Environmental Engineering, Indian Institute of Technology Tirupati, Tirupati- 517506, India*

(*Received August 6, 2019, Revised March 15, 2020, Accepted March 25, 2020*)

**Abstract.** Open ground story (OGS) reinforced concrete (RC) buildings are vulnerable to the complete collapse or severe damages under seismic actions. This study investigates the effectiveness of four different strengthening techniques representing the local and global modifications to improve the seismic performance of a non-ductile RC OGS frame. Steel caging and concrete jacketing methods of column strengthening are considered as the local modification techniques, whereas steel bracing and RC shear wall systems are selected as the global strengthening techniques in this study. Performance-based plastic design (PBPD) approach relying on energy-balance concept has been adopted to determine the required design force demand on the strengthening elements. Nonlinear static and dynamic analyses are carried out on the numerical models of study frames to assess the effectiveness of selected strengthening techniques in improving the seismic performance of OGS frame.. Strengthening techniques based on steel braces and RC shear wall significantly reduced the peak interstory drift response of the OGS frame. However, the peak floor acceleration of these strengthened frames is amplified by more than 2.5 times as compared to that of unstrengthened frame. Steel caging technique of column strengthening resulted in a reasonable reduction in the peak interstory drift response without substantial amplification in peak floor acceleration of the OSG frame.

**Keywords:** performance-based design; reinforced concrete frame; seismic retrofitting; strength; soft-story mechanism

## 1. Introduction

Reinforced concrete (RC) frames infilled with masonry walls are generally preferred in the construction of buildings in many developing countries. These frames with open ground story (OGS) configurations offer several functional and architectural advantages, such as, parking, garages, storage, and other commercial activities (Oinam and Sahoo 2019). However, most of the existing OGS buildings in Indian subcontinent are seismically deficient as they have not been designed and detailed for the expected lateral force demand (Jain *et al.* 2002, Bothara *et al.* 2017). The presence of masonry infill walls increases the lateral strength and lateral stiffness at any story of a RC frame. Infill walls uniformly distributed over the height of a multi-story frame (e.g., fully infilled frame) results in the significantly higher lateral strength and stiffness as compared to the bare RC frame. The absence of infill walls in any story level creates the stiffness discontinuity over the height of a RC frame. As a consequence, the frame members at that story level are subjected to very high interstory displacement demand. Similarly, members in stories with masonry infill walls experience small interstory displacement demand because of high lateral stiffness.

Under lateral loading, the behavior of stories with fully-infilled masonry walls is similar to that of a rigid body resulting in the amplified lateral force and displacement demand in the stories without infill walls. This leads to the concentration of plastic hinges (damages) in the weaker (i.e., without infill walls) stories, which is commonly known as ‘soft-story’ mechanism. Many RC buildings with such stiffness discontinuity have suffered severe damages or complete collapse even in low intensity earthquakes, if not designed and detailed considering the seismic load demand (i.e., Dolšek and Fajfar 2001, Saravanan *et al.* 2017). In the OGS RC frames, soft-story failure mechanism occurs at the ground story level. Further, torsional irregularity and in-plane discontinuity in vertical lateral force-resisting systems may lead to the progressive collapse of a structure under seismic loading (Yavari *et al.* 2019).

Strengthening schemes adopted to improve the seismic performance of a structure can be broadly classified into two categories, namely, local and global (Moehle 2000). Local strengthening schemes aim at modifying the section properties of frame members, thereby, improving their load-resisting capacity and displacement ductility. Examples of local strengthening schemes are steel caging, concrete jacketing, fiber reinforced polymer (FRP) wrapping. Global strengthening schemes involve either the enhancement in lateral strength and stiffness of structures through the installation of additional elements or the reduction in lateral force demand through the use of supplemental energy dissipation systems (Oinam and Sahoo 2016). Examples of global strengthening schemes are the bracings, shear walls, energy dissipation devices (Oinam 2017). Many of these

*Corresponding author, Associate Professor
E-mail: drsahoo@civil.iitd.ac.in
[a]Former M. Tech. Student
[b]Assistant Professor


http://www.techno-press.org/?journal=acc&subpage=7
ISSN: 2287-5301 (Print), 2287-531X (Online)

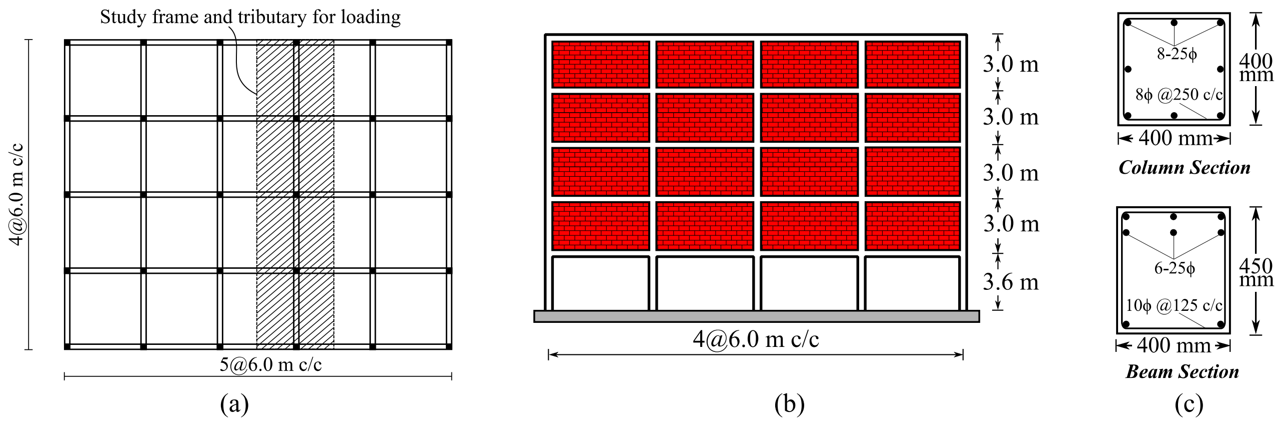


Fig. 1 Details of study frame: (a) Building plan, (b) frame elevation, and (c) dimensions of frame sections

techniques are being adopted in the practice for seismic strengthening of the non-ductile RC structures.

Dritsos (1997) proposed an upgrading technique for RC columns using external steel cage with pre-tensioned transverse ties. Test results showed the improved axial compressive strength and ductility of the upgraded columns as compared to the unstrengthened ones. A parametric study using finite element models was conducted by Adam *et al.* (2008) to investigate the behavior of axially loaded RC columns strengthened by steel caging. The use of steel tubes inside the beam-column joint regions and welded to the steel caging of columns improved the ultimate load of the beam-joint assembly. Cyclic testing of RC columns strengthened with steel caging exhibited the better lateral strength, displacement ductility, and energy dissipation capacity as compared to the unstrengthened RC columns (Nagaprasad *et al.* 2009). This technique is regarded as practical, fast, and cost-effective, which helps to improve the global seismic behavior of RC structures (Dritsos and Pilakoutas 1992, Garzon-Roca *et al.* 2011, Oinam and Sahoo 2016). This method has also been used in retrofitting of many damaged RC columns after the 2001 Bhuj Earthquake (Murty *et al.* 2005). In concrete jacketing technique, RC members are wrapped with a jacket of concrete reinforced with longitudinal steel bars and/or welded wire fabric (Alcocer and Jirsa 1993, Teran and Ruiz 1992). This increases the shear and flexural strengths of existing sections resulting in the enhancement in lateral stiffness and strength of frames (Júlio and Branco 2008, Vandoros and Dritsos 2008). This technique was adopted to retrofit most of the damaged RC beams and columns after the 1985 Mexico Earthquake (Teran and Ruiz 1992).

Concentrically braced steel frames are one of the most economical and effective lateral force-resting system used for strengthening RC structures in the regions of high seismicity. Steel braces undergo axial deformations in tension and compression to dissipate the hysteretic energy under cyclic loading (Kumar *et al.* 2017). However, the elastic compression buckling of steel braces may result in the extensive damage to the adjacent columns and beams (Karamodin and Zanganeh 2017). Similarly, RC shear walls significantly increase the lateral strength and stiffness of structures and can be used to strengthen the deficient structures in the high seismic regions. These walls are built continuously along the height of the building to effectively resist the lateral load (Wallace 1994). The high lateral stiffness of RC shear walls reduces the lateral sway and control the damage levels in the frame members (Motter *et al.* 2018). However, very limited studies have been conducted on the use of RC shear wall as strengthening technique in the structures.

Smyrou (2015) conducted a comparative study between FRP wrapping and column jacketing as strengthening techniques for a mid-rise RC building in Turkey. Chaulagain *et al.* (2015) numerically evaluated the effectiveness of different strengthening solutions in upgrading the seismic performance of existing RC buildings in Nepal using adaptive pushover and dynamic time history analyses. It was concluded that the retrofitting solutions, namely, RC shear wall, steel bracing, and RC jacketing improved the seismic performance of existing buildings and successfully met the standard drift limits as prescribed in the relevant building code. Srechai *et al.* (2017) developed a retrofitting technique for masonry-infilled non-ductile RC frame by providing a vertical gap between columns and infill panels. Shear force between the frame and masonry panels is allowed to transfer through additional structural steel elements. Ghobadi *et al.* (2019) studied the effectiveness of in-situ repair technique using infill masonry walls in improving the seismic performance of a damaged steel frame. Test results showed that the repair technique successfully restored the lateral stiffness and ductility of the steel frame. Though the strengthened elements are expected to undergo appreciable inelastic deformation under seismic loading, the current force-based design may not provide a cost-effective solution. Further, very limited studies have been conducted on the strengthening schemes to improve the seismic performance of soft-story RC buildings. Hence, this study is focused on a systematic evaluation and effectiveness of various seismic strengthening techniques for soft-story OGS RC buildings.

## 2. Research objectives

The conventional seismic design procedure involves the estimation of lateral force demand to achieve the desired structural performance by allowing the controlled damage

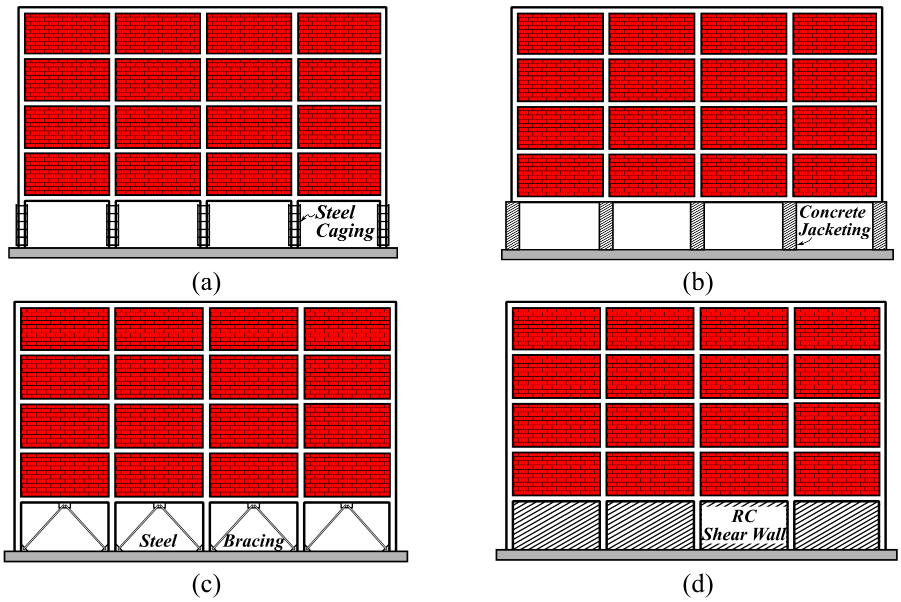


Fig. 2 Schematic representation strengthening schemes: (a) Steel caging, (b) Concrete jacketing, (c) Steel bracing, (d) RC shear wall

in frame members at the selected locations. Since the damage of a member is directly related to the displacement, rather than force, the current force-based design method may not provide the economical design as well as the desired performance of the strengthened frame under seismic loading. The primary objectives of this study are to develop a design methodology for the strengthened frame in the context of performance-based framework and to compare the seismic performance of the RC frames strengthened using different techniques. Four types of strengthening techniques representing the local and global modification schemes are considered for a non-ductile five story OGS RC building. Performance-based plastic design (PBPD) methodology has been adopted to determine the required size of strengthening elements. The main parameters considered for the comparison of seismic performance of strengthened frames are failure mechanism, interstory drift response and the floor acceleration. The details of study frame, modelling technique, and analysis methods used to evaluate the nonlinear behavior of the strengthened frames are discussed in the following sections.

## 3. Details of study frame

A five-story RC frame building with OGS configuration is considered in this study. An interior bay represented by the shaded region of the building plan, as shown in Fig. 1(a), is taken as the study frame. Fig. 1(b) shows the elevation of the study frame. The building is assumed to be located on rock site in the highest seismic zone-V of India (IS:1893-I 2016). This frame is designed only for the gravity loads without considering the seismic load demand. Dead load on each floor is assumed as 28.6 kN/m, whereas live loads on floor and roof levels are considered as 18.0 and 9.0 kN/m, respectively. Concrete of characteristic cube compressive strength of 20 MPa and Fe415 grade of steel reinforcing bars are used in the frame members. It is worth mentioning that concrete grades in many existing buildings in developing countries may be smaller than the value considered in this study. The specified values of yield stress, ultimate stress, and percentage of elongation of Fe415 grade steel bars are 415 MPa, 485 MPa, and 14.5%, respectively. Fig. 1(c) shows the dimensions and reinforcement details of beams and columns. It is assumed that same sizes of beams and columns are used in all story levels of the study frame.

Four strengthening techniques, namely, steel caging, concrete jacketing, steel bracing, and RC shear wall, are adopted in this study to evaluate their effectiveness under seismic loading conditions. The OGS configuration of the study frame allows the installation of additional strengthening elements in the ground story only. As shown in Figs. 2(a) and 2(b), all ground story columns of the study frame are strengthened using steel caging and concrete jacketing, respectively. In case of steel bracing system, concentrically steel braces in the chevron configurations are used in all bays of the ground story. These braces are connected at the mid-span of ground story beams and the column bases of the study frame as shown in Fig. 2(c). In the fourth case, RC shear walls are used only at the ground story level spanning over the entire bays of the frame as shown in Fig. 2(d). Steel caging technique is simple to implement, requires less cost, and results in the minimum loss of working space. The technique involving RC shear walls requires separate foundation and proper connection with the existing frame and consume the highest working space. It is worth mentioning that adding steel braces or RC shear walls in all the bays at the ground story of the RC frame may be unrealistic due to architectural reasons. In practice, only a few interior frames of a building can be utilized for this purpose. Nevertheless, such configurations have been considered in this study for the sake of comparison. A detailed procedure to determine the required sizes of strengthening elements using performance-based

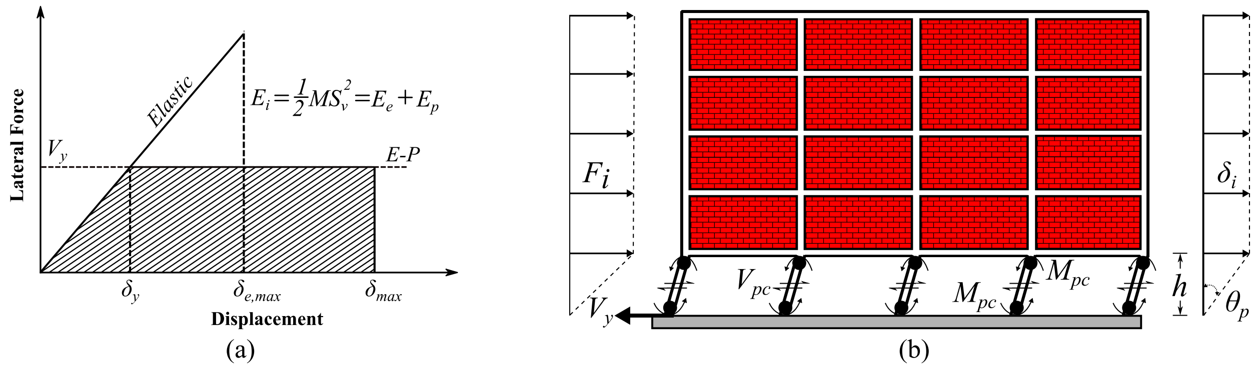


Fig. 3 (a) Energy balance concept for an elastic-perfectly plastic system and (b) assumed yield mechanism with displacement and force distribution over the height of OGS frame

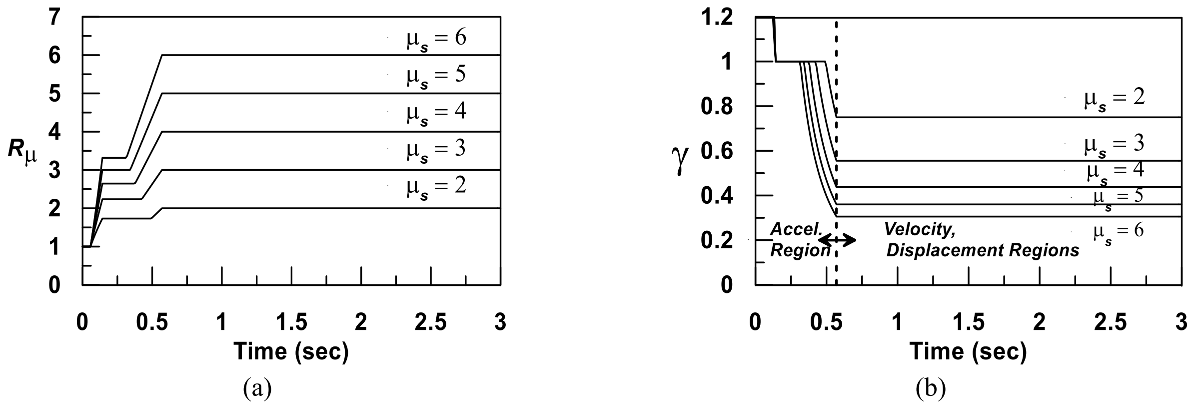


Fig. 4 Variation of (a) ductility reduction factor and (b) structural ductility factor with natural time periods

design approach has been presented in the following sections.

## 4. Strengthening of study frame

### 4.1 Design methodology

Performance-based plastic design (PBPD) method relies on the energy balance concept, which states that the amount of energy required for a structure to be monotonically pushed to a maximum target drift for pre-selected yield mechanism is equal to the input earthquake energy (Newmark and Hall 1982). Fig. 3(a) shows the energy balance concept for an elastic-perfectly plastic system. This procedure directly accounts for the inelastic behavior of structure in the design (Goel and Chao 2008). PBPD design methodology has been implemented successfully in the design of steel braced frame structures (Sahoo and Chao 2010, Goel *et al.* 2010) and RC buildings (Sahoo and Rai 2010, Liao 2010). Target yield drift, ultimate drift, and yield mechanism are the main parameters considered in this design method.

Fig. 3(b) represents the assumed yield mechanism for OGS frame, in which all plastic hinges are concentrated only in the ground story columns and the members in the upper stories remain elastic. The design yield base shear of a system as per PBPD method can be expressed as follows (Goel and Chao 2008)

$$\frac{V_y}{W} = \frac{-\alpha + \sqrt{\alpha^2 + 4S_a^2\left(\gamma/\eta\right)}}{2} \tag{1}$$

Where, $V_y$=design yield base shear, $W$=total seismic weight, $\gamma$=energy modification factor, $\eta$=factor to account for pinched hysteretic behavior, $\alpha$ =dimensionless parameter depending on fundamental time period, $T$ and is equal to ${8\theta_p h}/{T^2}$, where $h$=height of ground story and $\theta_p$=plastic rotation.

For the OGS building, the values of yield drift, $\theta_y$ and ultimate drift, $\theta_u$ are taken as 0.2% and 2.0%, respectively (Oinam 2017). Assuming the plastic rotation of frame sections is nearly same as the inelastic drift of a member, the value of $\theta_p$ $(= \theta_u - \theta_y)$ is computed as 1.8%. Liao (2010) proposed the value of $\eta$ equal to 0.2 for the RC frames. Energy modification factor, $\gamma$ can be determined from structural ductility factor, $\mu_s$, and the ductility reduction factor, $R_\mu$ using $R - \mu - T$ relationship (Fig. 4).

Seismic input energy, $E_i$ and dissipated energy, $E_d$ can be calculated as follows (Sahoo and Rai 2010)

$$E_i = \frac{\gamma W S_a{}^2 T^2}{8} \tag{2}$$

$$E_d = 2\left(\theta_p + \theta_y\right)M_{pc}n_c \tag{3}$$

Where, $S_a$=period-based spectral acceleration; $M_{pc}$=moment capacity of column and $n_c$=number of

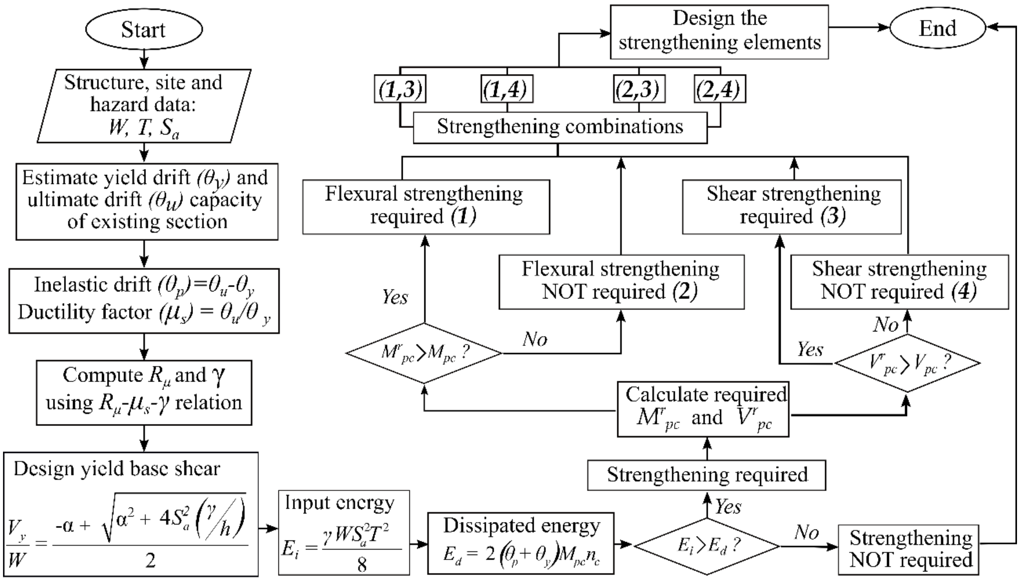


Fig. 5 Step-by-step procedure for the evaluation and strengthening of existing building using PBPD method

ground story columns. Eq. (3) is derived based on the assumption that flexural plastic hinges are only formed at both ends of all ground story columns (soft-story mechanism). A need to strengthen a structure arises when the input seismic energy demand is higher than its energy dissipation potential.

Fig. 5 shows a step-by-step procedure for the evaluation and strengthening in accordance with PBPD methodology. The same procedure has been adopted for evaluation of the frame considered in this study. All ground story columns are found to be deficient in terms of flexural and shear capacities for the lateral force demand computed in accordance with Indian Standard IS:1893-I (2016) provisions. An interstory drift of 2.5% is considered as the acceptable performance for the RC frame (ACI 374.1-05 2005). In this study, the target inelastic drift, $\theta_p$ $(= \theta_u - \theta_y)$ for the OGS RC frame is taken as 1.5% conservatively. Accordingly, the yield base shear ratio $(V_y/W)$ for the unstrengthened frame is computed as 0.335 and the design yield base shear of the frame is found to be 1987.1 kN. Assuming soft-story mechanism, the required flexural and shear strengths of ground story columns are computed as 500.6 kNm and 397.4 kN, respectively. The yield moment capacity and shear capacity of these columns are determined as 197.0 kNm, and 186.5 kN, respectively. Both steel caging and concrete jacketing techniques are adopted to improve the flexural and shear strengths of columns.

### 4.2 Design of steel cage

Steel caging technique is adopted to enhance the axial, shear and flexural capacities of ground story columns. Steel cage is designed to satisfy the deficit moment capacity of 303.5 kNm following the same procedure as proposed by Nagaprasad *et al.* (2009). The material yield and ultimate strengths of steel angles and battens are taken as 250 MPa and 380 MPa, respectively. The required area of steel cage is estimated as 1517 mm$^2$. Four Indian Standard steel angle sections ISA 80×80×12 (area=1781 mm$^2$) are selected as the longitudinal members of steel cage. Mild steel plates of size 350×10 mm are used as battens at a spacing of 200 mm on centers. The shear capacity of steel cage is computed as 257 kN. Total shear strength of the strengthened column is determined as 443.3 kN, which is higher than the required strength of 397 kN. The details of steel cage strengthened column are shown in Fig. 6(a).

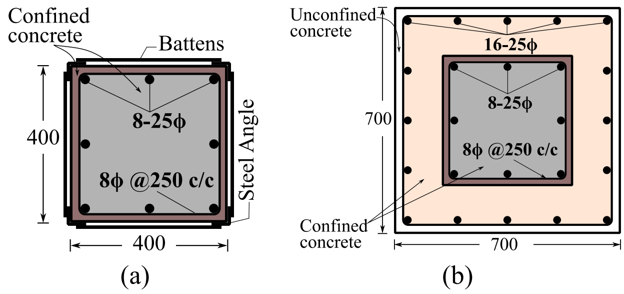


Fig. 6 Strengthened column sections: (a) Steel caging, (b) Concrete jacketing
(Note: All dimensions are in millimeters)

### 4.3 Design of concrete jacketing

For concrete jacketing of columns, the shear demand is determined based on the input seismic energy demand, $E_i$. Assuming the value of $\mu_s$ as 3.0 for the RC frame having the natural period of 0.62 sec., the value of $\gamma$ can be determined as 0.58 using Fig. 4. Period-based spectral acceleration factor $(S_a)$ is found to be 1.61 (IS:1893-I 2016). Accordingly, the value of $E_i$ is computed as 430.9 kNm using Eq. (2). Shear demand on columns is computed assuming the energy dissipated by the shear plastic hinges formed at both ends of all ground story columns. Mathematically

$$V_{pc} = \frac{E_i}{2n_c(0.5\delta_{yv} + \delta_{uv})} \tag{4}$$

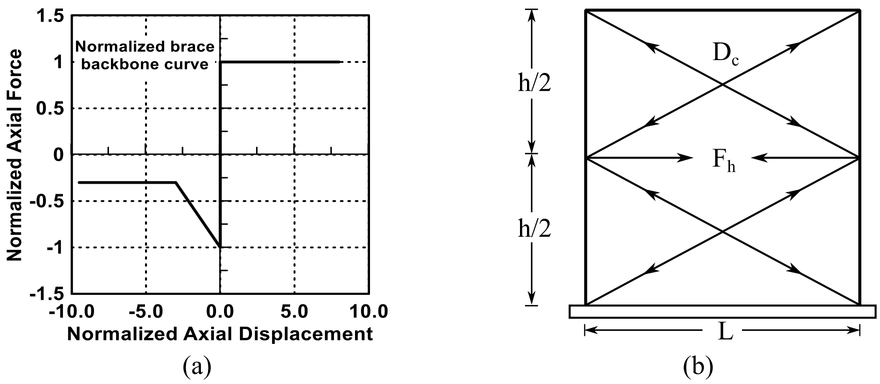


Fig. 7 (a) Force-deformation behavior of steel braces, (b) Strut-and-tie modelling of RC shear wall

Where, $\delta_{yv}$ and $\delta_{uv}$ are the yield and ultimate shear displacements of column sections, which are assumed as 0.05 m and 0.5 m, respectively (Kato and Ohnishi 2001). The required shear strength of column is calculated as 548.7 kN. Accordingly, the shear force to be resisted by the concrete jacketing is estimated as 362.6 kN.

Fig. 6(b) shows the details of column sections strengthened using concrete jacketing. The overall size of strengthened column is taken as 700×700 mm, which is reinforced with 16 numbers of 25 mm diameter bars as additional longitudinal reinforcement and 8 mm diameter bars as transverse stirrups at 250 mm on centers. Shear strength of the strengthened column is computed 561.8 kN. It is worth mentioning that the use of additional longitudinal reinforcing bars would significantly increase the flexural strength of columns at their bases provided that these bars are anchored to the column footing properly. In such cases, the failure of these columns would be governed by the formation of shear hinges. Therefore, the flexural strength enhancement due to concrete jacketing has not been considered in the design.

### *4.4 Design of steel bracing*

Both compression buckling and tension yield strengths are considered for the computation of hysteretic energy capacity of steel braces (Bruneau *et al.* 2011). After the compression buckling, axial force demand on tension braces in a braced frame is suddenly increased resulting in the initiation of tension fracture. This behavior of braces is taken into account in the design of steel bracings for strengthening of the study frame. Yield and ultimate drifts of bracing systems are considered as 0.36% and 2.5%, respectively (Reza Banihashemi *et al.* 2015). Accordingly, the value of $\mu_s$ is computed as 6.9. Fundamental time period of the RC frame strengthened using steel bracings is considered as 70% of the original RC frame, i.e., $T$=0.43 sec. The value of $\gamma$ is computed as 0.27. Thus, the design yield base shear ($V_y$) for the strengthened frame is computed as 1040 kN.

Hollow square steel (HSS) sections of 5×5×3/8 mm size are chosen as braces having the slenderness ratio of 98.5. The material yield and ultimate stresses of HSS section are assumed as 317 MPa and 400 MPa, respectively. Tensile and buckling strengths of braces are computed as 1391.0 kN and 754.3 kN, respectively, considering the slenderness ratio and width-to-thickness ratio of braces. The post-buckling strength of brace is considered as 30% of the peak compressive strength (Sabelli *et al.* 2003). Fig. 7(a) shows the idealized axial force *vs.* axial deformation behavior of braces, in which the magnitudes of force and deformation are normalized with respect to their respective yield values. Shear strength contribution of braces can be estimated by resolving the tension and compression axial strengths along the direction normal to the longitudinal axes of columns. Considering the shear strengths of RC columns and braces, total shear capacity of the strengthened frame is computed as 1372.4 kN, which is higher than the required design value of 1040 kN.

### *4.5 Design of RC shear wall*

RC shear wall of 230 mm thickness spanning over the entire bay width of the RC frame is considered at the ground story level. Usually, truss model is adopted to represent the lateral strength stiffness of slender shear walls due to its simplicity and less computational effort. In such models, the state of stresses in the central panel is assumed to be uniform and the flow of compressive stresses is idealized by a series of parallel compressive struts. In RC shear walls of low aspect ratios, the top and bottom regions are subjected to the high internal stresses due to presence of concentrated loads as compared to those in the central regions. Considering this uneven distribution of internal stress, strut- and -tie model is used for the low-rise RC shear wall instead of the truss model. In strut and tie model, the compressive struts depict the flow of concentrated compressive stresses in the concrete and tension ties represent the reinforcing steel.

Fig. 7(b) shows the strut and tie model adopted in this study to represent the lateral strength and stiffness of RC shear wall. It consists of two flat struts and one equivalent horizontal tie. Width of diagonal strut is computed as 1190 mm (Paulay and Priestley 1992). Characteristic compressive strength of concrete is assumed as 20 MPa. The equivalent area of horizontal bar is computed as 5542 mm$^2$ carrying an average tensile force of 2230 kN. The compressive force in the inclined strut is computed as 34030 kN. The contribution of horizontal and vertical web reinforcement bars is ignored in the computation of lateral

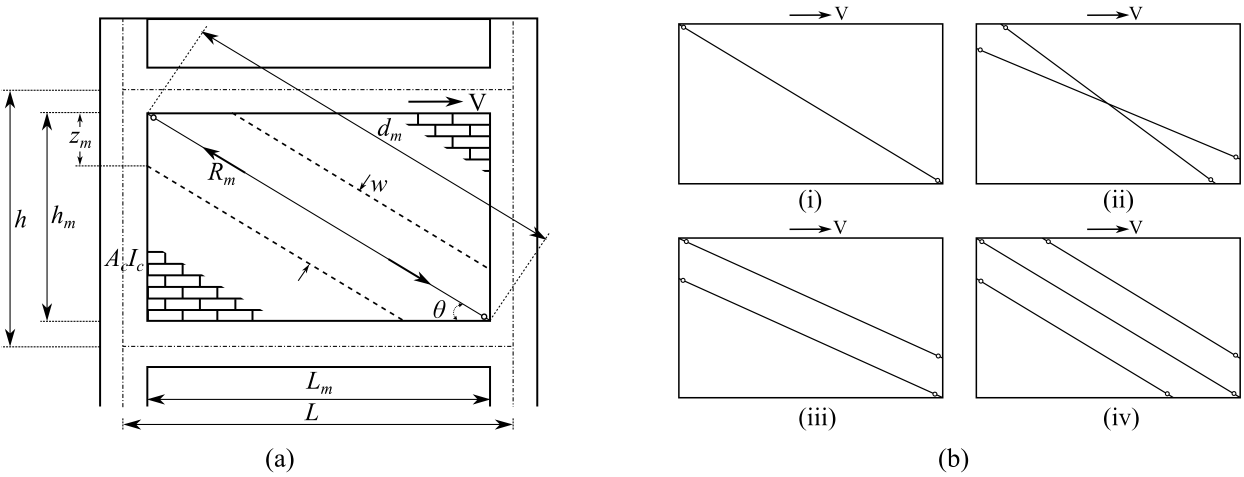


Fig. 8 (a) Effective width of masonry strut, (b) various strut configurations used in modelling of masonry panels

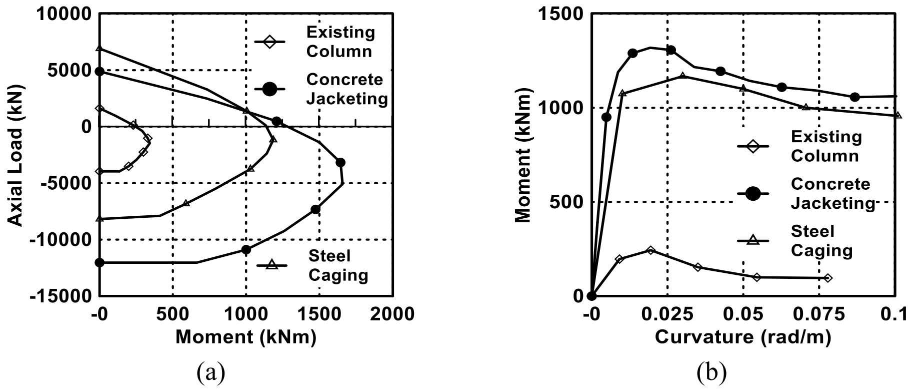


Fig. 9 Comparison of section properties of columns: (a) *P-M* interaction , (b) *M-φ* response

strength of RC shear wall. The lateral strength of RC shear wall is computed using the strut and tie model (Hwang *et al.* 2001).

## 5. Numerical modelling

A computer program SAP2000 (CSI, 2017) is used to numerically investigate the seismic behavior of the study frames. All members are modelled as two-node frame elements incorporating their axial, shear and flexural characteristics. For nonlinear analysis, lumped plasticity model has been adopted with discrete plastic hinges assigned at the pre-determined locations in the members. Flexural behavior is modelled as deformation-controlled action, whereas shear and axial behaviors are considered as force-controlled actions. Axial force-bending moment (*P-M*) hinge and shear hinges are assigned to columns, whereas the moment-curvature (*M-φ*) hinges and shear hinges are assigned to beams of the study frame. Fig. 8(a) shows the width of masonry panel effective in resisting the lateral load by strut action. Width of masonry panels is computed in terms of infill-frame stiffness parameter, $\lambda_h$ as follows (FEMA 306 1998)

$$\lambda_h = \sqrt[4]{\frac{E_m t_{inf} \sin 2\theta}{4 E_c I_c h_m}} \tag{5}$$

Where, $E_m$ and $E_c$ are the modulus of elasticity of masonry and frame material, respectively, $h_m$ is height of infill panel, $I_c$ is moment of inertia of column, $t_{inf}$ is thickness of infill panel, and $\theta$ (radians) is angle between the infill height and infill length. Effective width of strut, $w$ can be calculated as follows

$$w = 0.175\left(\lambda_h h\right)^{-0.4} d_m \tag{6}$$

Where, $h$ is the column height between centerlines of beams and $d_m$ is diagonal length of infill panel.

Fig. 8(b) shows the various configurations of strut models, namely, single strut (i), double struts (ii,iii) and three struts (iv), often considered to represent the strength and stiffness of masonry panels. In single strut model, beams and columns are subjected to the higher rotational demands than expected in the practice. Three strut model has shown to provide a realistic behavior of frame under lateral loading by distributing the internal stresses over a wider diagonal (Oinam and Sahoo 2018). In this study, both single and three strut models have been adopted to model masonry infill wall for numerical study. Axial load-bending moment (*P-M*) interaction and moment-curvature (*M-φ*) characteristics at zero axial force level of the existing and strengthened columns are shown in Fig. 9. The strengthened columns exhibited the significantly higher axial and flexural strengths using steel caging and concrete jacketing. Axial plastic hinges are considered for the modelling of nonlinear

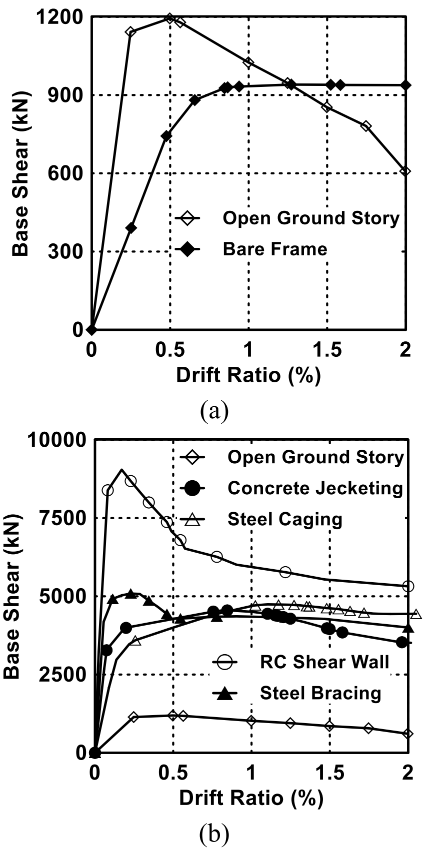


Fig. 10 Comparison of capacity curves: (a) Unstrengthened frames, (b) Strengthened frames

behavior of masonry infill walls and braces.

## 6. Evaluation of seismic performance

Both nonlinear static (pushover) and dynamic analyses are conducted to evaluate the seismic performance of the Unstrengthened and strengthened OGS fames. The results of these analyses are discussed in the following sections:

### *6.1 Pushover analysis*

Non-linear static analysis is performed by gradually increasing the lateral displacements in displacement-controlled mode till 2.0% lateral drift. The fundamental mode shapes of the study frames are considered as the displacement profiles in the pushover analysis. The main parameters investigated in this study are the damage state, yield mechanism, drift capacity and lateral load carrying capacity of the existing and strengthened frames.

#### *6.1.1 Capacity curves*

Fig. 10(a) shows the lateral strength-roof displacement (capacity) curves of the OGS frame and bare RC frame (i.e., without any infill walls at any story level). The OGS frame exhibited the higher lateral strength and stiffness as compared to the bare RC frame. The yielding drifts of the bare frame and the OGS frame are noted as 0.49% and 0.24%, respectively. The peak lateral strengths of these

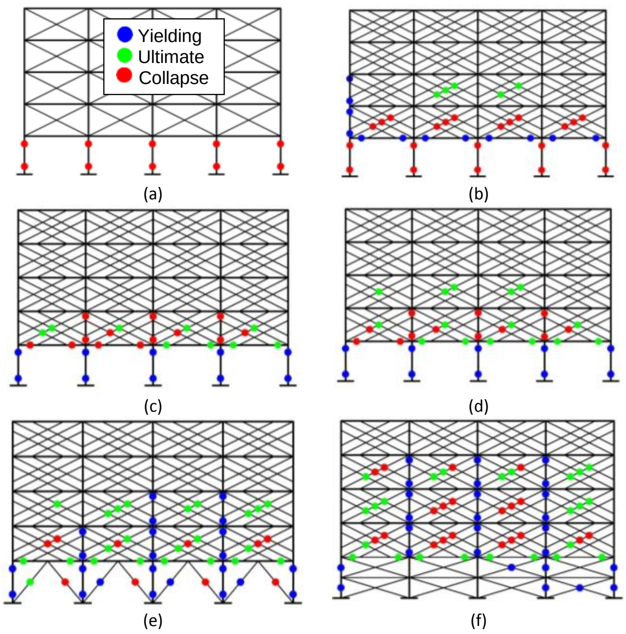


Fig. 11 Hinge mechanism: (a) OGS frame with single strut, (b) OGS frame with multi-struts, (c) Steel caging, (d) Concrete jacketing, (e) Steel bracings, (f) RC shear wall

frames are observed as 940.2 kN and 1193.6 kN, respectively. The post-peak lateral strength of the OGS frame is reduced rapidly, as evident from the negative slope, indicating its sudden failure as compared to that of the bare RC frame. The post-peak behaviour of RC bare frame is found to be more ductile without any strength-reduction till a lateral drift of 2%.

Fig. 10(b) shows the comparison of capacity curves of the strengthened frames with the original OGS frame. All strengthened frames exhibited the higher lateral stiffness and strength as compared to the OGS frame. The maximum increase in the lateral stiffness and strength is noted in the frame strengthened using RC shear wall. The peak lateral strengths of the OGS frame strengthened using steel cage, concrete jacketing, steel bracings, and RC shear wall frame are noted as 4740.9, 4550.3, 5087.2 and 9043.5 kN, respectively. Both steel cage and concrete jacking techniques exhibited the nearly same peak lateral strengths. A significant reduction in the post-peak lateral strength is noted in the frame strengthened using RC shear wall. Similar reduction in lateral strength is also noted in the OGS frame with steel bracings. The OGS frame with steel cage columns exhibited the better post-peak lateral strength and displacement ductility.

#### *6.1.2 Yield mechanism*

In order to investigate the role of modelling technique, two analysis cases are considered for the OGS frame in which the masonry infill walls modelled using single strut or three struts. As shown in Figs. 11(a)-(b), all ground story columns of the OGS frame exhibited the plastic hinges at both ends and reached their collapse limits in both cases. In Fig. 11, yielding point corresponds to a point where a member reached its yielding strength. Ultimate state in hinge mechanism represents that the member reached the

Table 1 Details of selected ground motions

| Earthquake | Recording Station | PGA (g) | Richter Magnitude | Distance (km) | Duration (sec) |
|---|---|---|---|---|---|
| Gorkha (2015) | Kantipath, Kathmandu | 0.25 | 7.8 | 8.2 | 100 |
| Imperial Valley (1940) | El Centro | 0.34 | 6.9 | 16 | 53.76 |
| Koyna Dam #06 (1967) | Koyna Dam, 1A Gallery | 0.48 | 6.6 | 12 | 10.72 |
| Mammoth Lakes (1980) | Convict Creek | 0.39 | 6 | 10.5 | 65 |
| Morgan Hill (1984) | Halls Valley | 0.31 | 6.2 | 10 | 60 |
| San Salvador (1986) | Inst. Urban Construction | 0.38 | 5.7 | 10 | 11.54 |
| Whittier (1987) | Obregon Park | 0.42 | 6.1 | 14.2 | 40 |

ultimate (peak) strength. Similarly, collapse point corresponds to a state where the member reached the maximum rotational capacity in the post-peak strength-reduction stage. The failure of all ground story columns of the OGS frame is noted due to inadequate shear and flexural strengths. In case of numerical model with three-strut models of masonry infill, yielding of beams at the first story level and columns in the upper stories are also noted at the failure stage. This failure mechanism is consistent with the observed behavior of the OGS frame in the past earthquakes (Jain *et al.* 2002). Therefore, three strut modeling approach has been adopted for the masonry infill panels in the numerical models of all strengthened frames used in the nonlinear dynamic analyses.

The strengthening of ground story columns using the steel caging and concrete jacketing techniques significantly increased the flexural/shear strength and the plastic rotational capacity. This eliminated the collapse of ground story columns though these columns reached their yielding limits as shown in Figs. 11 (c)-(d). The first-story beams and interior columns reached their failure limits due to the propagation of damage from the ground to upper stories. The same mode of failure is noted in both strengthened frames. This also highlighted the requirement of additional strengthening strategy at the global level to further improve seismic performance.

In the strengthened frame with global modifications (i.e., steel bracings and RC shear wall), the primary members of the RC frame did not reach their collapse limits states as shown in Figs. 11 (e)-(f). Column yielding is noted in the top stories though they did not reach their ultimate stages. Plastic hinges in beams reached their ultimate limits. The damage to the infill walls is also noted in the top stories. As expected, tension yielding and compression yielding of braces are noted in the steel bracing system. The behaviour of RC shear wall is found to be essentially elastic as minor yielding of two struts is noted at the ground story level of the strengthened frame. The high lateral stiffness contribution of the steel bracings and RC shear walls resulted in the reduced the plastic rotation and lateral force demand on ground columns leading to the distribution of damage over the height of the strengthened frame. The hinge mechanisms of strengthened frames with steel

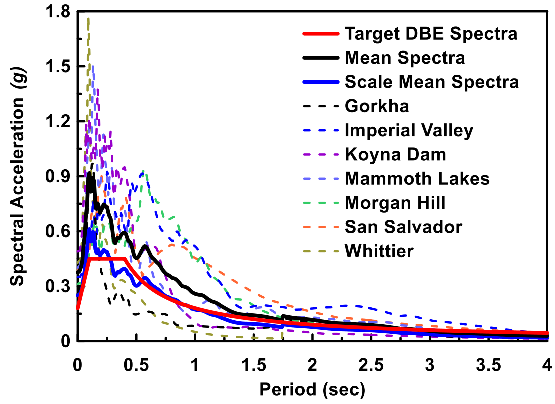


(a)

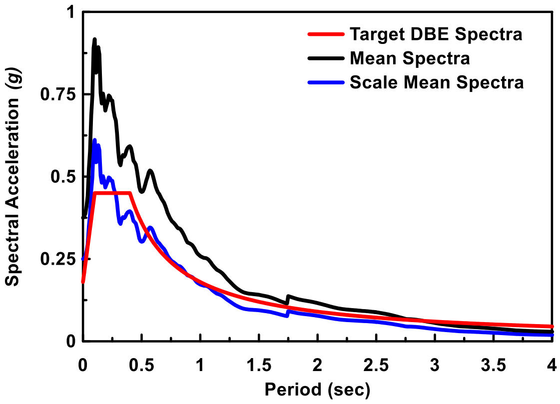


(b)

Fig. 12 Comparison of (a) unscaled response spectra and (b) scaled mean response spectra of selected ground motions

bracings as well as RC shear wall exhibited the yielding of columns and beams at the ground story. As compared to columns, beams are subjected to the higher plastic rotational demand. The upper story columns of these strengthened frames experienced very minor yielding, which can be considered to be negligible. Thus, it can be concluded that the mode of failure is consistent with the strong column-weak beam philosophy.

### *6.2 Time history analysis*

A set of seven recorded ground motions has been selected for the nonlinear time-story analyses of the study frames. Table 1 summarizes the details of selected ground motions. The peak ground acceleration (PGA) of the selected ground motions is nearly about 0.36 g, the value corresponds to the seismic zone -V as per IS:1893-I (2016). Fig. 12(a) shows the comparison of response spectra of all selected ground motions and the target design spectrum (IS:1893-I 2016). These ground motions are amplitude scaled in accordance with ASCE 7-10 (2010) guidelines which require that the average (mean) response spectrum obtained from at least five recorded or simulated acceleration-time histories response spectra should approximately match with the design spectrum over the period range of $0.2T$ to $1.5T$, where $T$ is the natural period of the considered structure. The mean spectrum of response spectra of set of all seven acceleration time history data has

Table 2 Details of plastic hinges formed in ground story columns of the OGS frame

| Ground motion | Shear hinging | Max. plastic rotation (rad) | Damage index | Time (sec) |
|---|---|---|---|---|
| Koyna Dam | All | 0.0032 | 0.40 | 3.42 |
| Imperial Valley | All | 0.0049 | 0.61 | 7.45 |
| San Salvador | All | 0.0043 | 0.54 | 1.04 |
| Mammoth Lake | All | 0.0026 | 0.33 | 8.08 |
| Morgan Hill | All | 0.0015 | 0.19 | 2.02 |
| Whittier | All | 0.0022 | 0.28 | 3.88 |
| Gorkha | Two columns | 0.0027 | 0.34 | 3.01 |

been reduced down to match with design basis earthquake (DBE) response spectrum obtained for seismic zone-V (IS:1893-I 2016) as shown in Fig. 12(b).

Table 2 summarizes the plastic hinge formation in ground story columns of the OGS frame under the selected ground motions. Both flexural and shear hinges are formed in columns of the OGS frame. Columns reached their ultimate shear capacities. Damage index is defined as the ratio of maximum plastic rotational demand to the ultimate plastic rotational capacity. The value of damage index equal to 0 represents no damage (or yielding), whereas the value equal to 1 corresponds to the complete flexural failure. As summarized in Table 2, the maximum value of damage index is noted as 0.61 in Imperial valley ground motion considering the ultimate plastic rotational capacity of columns is 0.008 rad. This shows that columns did not reach their ultimate flexural capacity at the failure stage. Thus, the OGS frame collapsed due to inadequate shear strengths of ground story columns. The failure of OGS frame is noted within 10 seconds of ground motion durations for all earthquakes.

The main parameters investigated are yield mechanism, peak interstory drift response and peak floor acceleration response of the study frames as discussed below.

#### *6.2.1 Peak floor displacement response*

Fig. 13 shows the floor displacement response of the unstrengthened and strengthened frames. The maximum floor displacement response of the bare frame is recorded as 0.7% lateral drift at roof level under the San Salvador earthquake. The peak displacement profile is found to be uniform over the height of the bare frame. In case of OGS frame, the maximum displacement is noted as 0.4% lateral drift at first floor level under the Morgan Hill earthquake. As compared to the unstrengthened frame, all strengthened frames exhibited the low lateral drifts under all ground motions. Strengthened frames with steel caging, concrete jacketing, steel bracing, and RC shear wall exhibited the lateral drifts of 0.2, 0.17, 0.11 and 0.08%, respectively. The average roof drift of the OGS frame is reduced by 49.2, 61.8, 84.1, and 88% using steel caging, concrete jacketing, steel bracing, and RC shear walls, respectively.

#### *6.2.2 Inter story drift response*

Fig. 14 shows the inter-story drift ratio (IDR) response of all study frames. The RC bare frame and the OGS frame showed the maximum IDR response of 1.0 and 1.3% at ground floor level under the San Salvador earthquake. This indicates that the maximum damage to the frame members

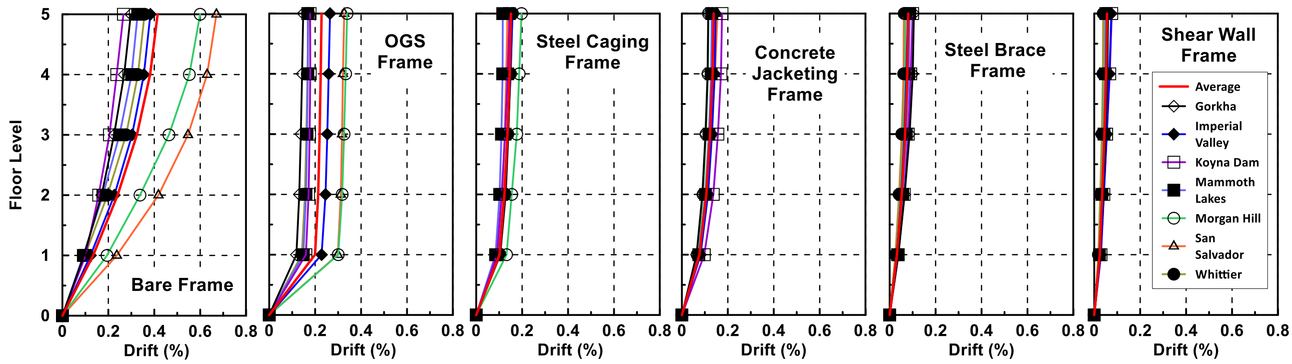


Fig. 13 Peak floor displacement response of study frames

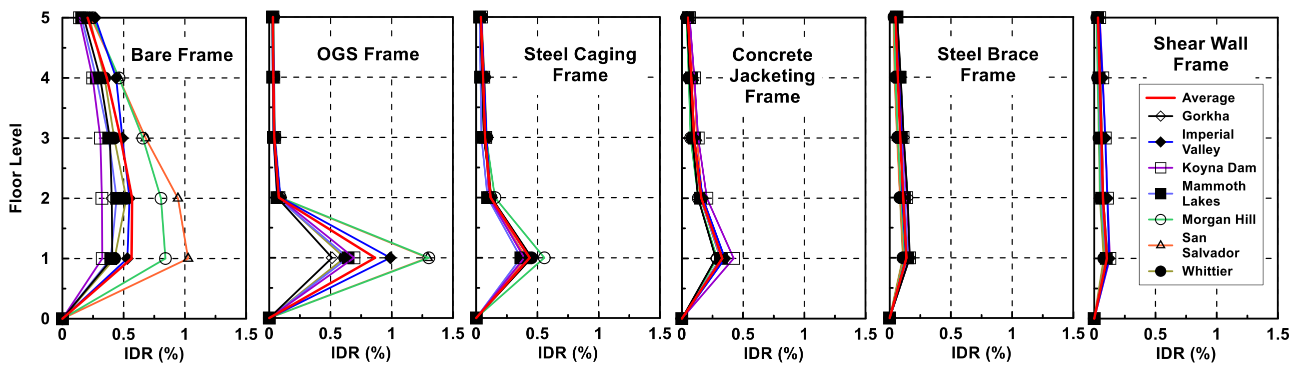


Fig. 14 Peak interstory drift ratio response of study frames

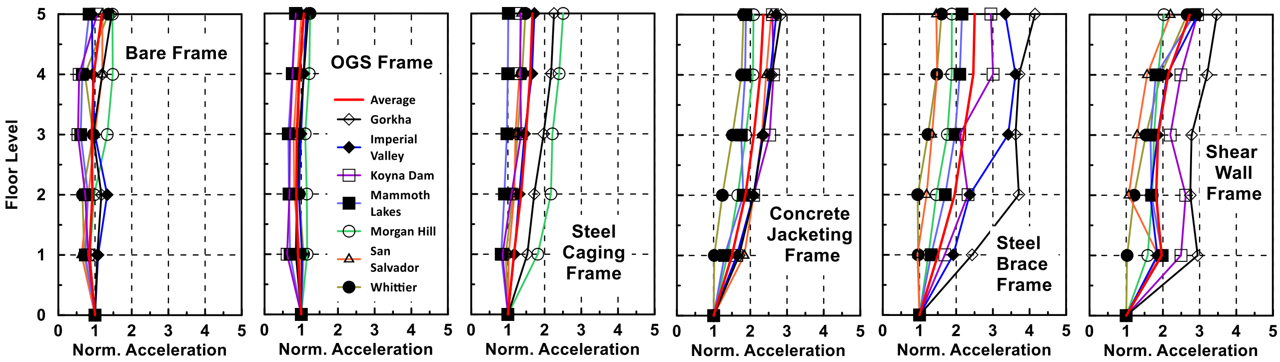


Fig. 15 Peak floor acceleration response of study frames

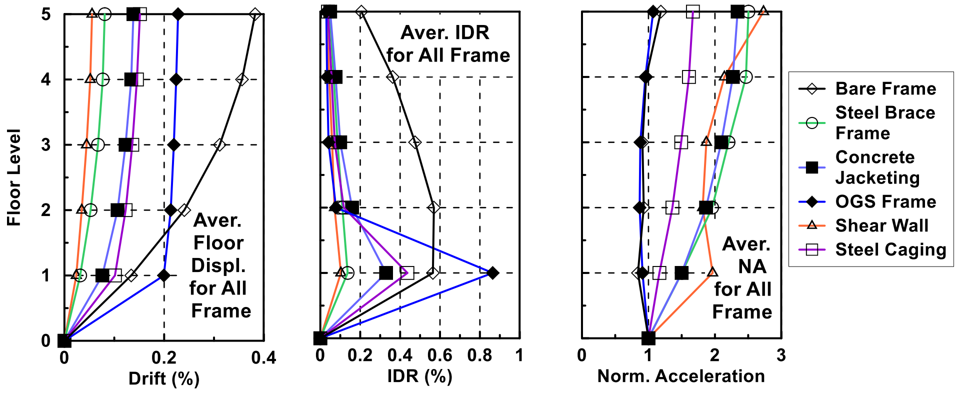


Fig. 16 Comparison of mean roof drift, IDR and normalized acceleration response of study frames

is noted at the lower stories as compared to those at the upper stories. The average values of peak IDR are recorded as 0.56, 0.42, 0.16, and 0.13% for the steel cage, concrete jacketing, steel bracing, and RC shear wall systems, respectively. Both steel caging and concrete jacketing techniques resulted in the reduced peak interstory displacement. These strengthened frames exhibited the similar displacement profile as that of the OGS frame. A more uniform displacement profile is noted for the frame strengthened using steel bracing and RC shear wall.

### *6.2.3 Floor acceleration response*

Fig. 15 shows the peak floor acceleration response of the unstrengthened and strengthened frames under the selected ground motions. The observed peak values of floor acceleration of study frames are normalized with respect to the corresponding PGA values of the ground motions. For the OGS frame, the roof acceleration is nearly same as that noted at the ground story level. All the strengthened frames except the steel caging technique, the roof acceleration is amplified by at least 2 times of the acceleration at the ground story level. The amplified roof acceleration for the frame strengthened using steel caging is noted as 1.66 times the value at the ground story level. The corresponding values of the strengthened frame with concrete jacketing, steel bracing and shear wall are noted as 2.34, 2.50 and 2.73. The amplified roof acceleration for the frames with steel bracings and RC shear wall is attributed to their increased lateral stiffness as compared to the other frames.

### *6.3 Discussion*

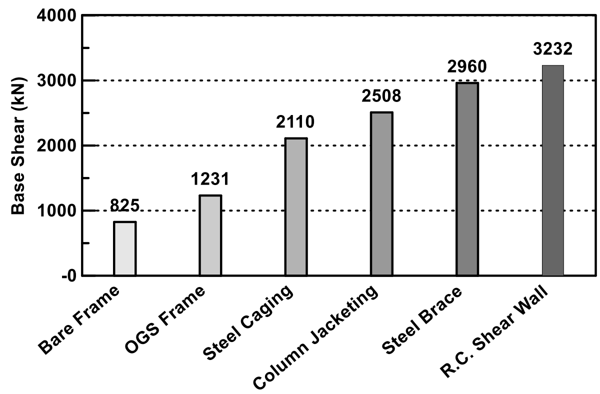


Fig. 17 Peak base shear demand in study frames

Fig. 16 shows the comparison of average response of all study frames under the selected ground motions. The bare RC frame exhibited the higher roof drift response, whereas the OGS frame exhibited the higher IDR response at the ground story level. However, the minimum level of amplification of floor acceleration is noted in both these frames. Similarly, the strengthened frames with steel bracings and RC shear wall controlled the excessive displacement response of the OGS frame, whereas the floor acceleration is amplified by more than 250%. Steel caging technique controlled the excessive drift response with minimum level of amplification of floor acceleration. On the other hand, the strengthened frame with concrete jacketing reduced the displacement response similar to that of the steel caging. However, the magnitude of amplified floor acceleration in this frame is noted same as that of with the steel bracing.

Fig. 17 shows the average values of base shear for the study frames as observed in time-history analyses. The base shear values are increased by 71.4%, 103.7%, 140.5% and 162.6% for the strengthened frames with steel caging, concrete jacketing, steel bracing and RC shear wall, respectively, as compared to that of the OGS frame. A higher the base shear demand would result in the higher foundation cost in addition to the cost of the strengthening elements and their installation. Hence, the cost-benefit analysis should be carried out to finalize a particular strengthening technique among all possible choices as applicable to a specific project.

## 7. Conclusions

The main conclusions drawn from this study are as follows:

- Both local and global strengthening techniques considered in this study exhibited their efficiency in controlling the excessive drift response and the complete collapse of the OGS frames. The study frames with ground story columns strengthened by steel caging or concrete jacketing exhibited nearly similar drift response. Similarly, the behavior of frames with global modifications (i.e., RC shear wall and steel bracings) is found to be nearly similar.
- The design of strengthening techniques using the performance-based plastic design method is found to be successful in improving the seismic performance of the non-ductile OGS RC frames.
- The increased lateral stiffness of the strengthened frames with global modification resulted in the amplified floor acceleration more than 250% of the input ground accelerations. The strengthened frame with steel caging of columns exhibited the reduction in the drift response as well as the minimum amplification in the floor acceleration.
- The concrete jacketing of ground story columns of the OGS frame though helped in controlling the excessive drift response resulted in the high amplification of floor acceleration.

## References

ACI 374.1-05 (2005), Acceptance Criteria for Moment Frames Based on Structural Testing and Commentary (ACI 374.1-05), American Concrete Institute, Farmington Hills, MI, U.S.A.

Adam, J.M., Ivorra, S., Pallares, F.J., Giménez, E. and Calderón, P.A. (2008), "Column-joint assembly in RC columns strengthened by steel caging", *Proc. Inst. Civil Eng.: Struct. Build.*, **161**(6), 337-343. https://doi.org/10.1680/stbu.2008.161.6.337.

Alcocer, S.M. and Jirsa, J. (1993), "Strength of reinforced concrete frame connections rehabilitated by jacketing", *ACI Struct. J.*, **90**(3), 249-261.

ASCE 7-10 (2010), Minimum Design Loads for Buildings and other Structures, American Society of Civil Engineers, Reston, Virginia.

Bothara, J., Dizhur, D., Dhakal, R. and Ingham, J. (2017), "Context and issues during post-earthquake rapid evaluation of buildings after the 2015 Nepal (Gorkha) earthquake", *Proceedings of SESOC Conference*, Wellington, New Zealand.

Bruneau, M., Uang, C.M. and Sabelli, R. (2011), *Ductile Design of Steel Structures*, McGraw-Hill, New York.

Chaulagain, H., Rodrigues, H., Spacone, E. and Varum, H. (2015), "Assessment of seismic strengthening solutions for existing low-rise RC buildings in Nepal", *Earthq. Struct.*, **8**(3), 511-539. http://dx.doi.org/10.12989/eas.2015.8.3.511.

CSI (2017), SAP2000 Analysis Reference Manual, Computers and Structures, Inc., Berkeley, California.

Dolšek, M. and Fajfar, P. (2001), "Soft-storey effects in uniformly infilled reinforced concrete frames", *J. Earthq. Eng.*, **5**(1), 1-12.

Dritsos, S. and Pilakoutas, K. (1992), "Composite technique for repair/strengthening of RC members", *Proceedins of the Second International Symposium on Composite Materials and Structues*, Beijing, China.

Dritsos, S.E. (1997), "Jacket retrofitting of reinforced concrete columns", *Constr. Repair*, **11**(4), 35-40.

FEMA 306 (1998), Evaluation of Earthquake Damaged Concrete and Masonry Wall Buildings Basic Procedures Manual, Applied Technology Council, Washington, DC.

Garzon-Roca, J., Adam, J.M. and Calderon, P.A. (2011), "Behaviour of RC columns strengthened by steel caging under combined bending and axial loads", *Constr. Build. Mater.*, **25**(5), 2402-2412. https://doi.org/10.1016/j.conbuildmat.2010.11.045.

Ghobadi, M.S., Jazany, R.A. and Farshchi, H. (2019), "In-situ repair technique of infill masonry walls in steel frames damaged after an earthquake", *Eng. Struct.*, **178**, 665-679. https://doi.org/10.1016/j.engstruct.2018.10.022.

Goel, S.C. and Chao, S.H. (2008), *Performance-based Plastic Design: Earthquake-resistant Steel Structures*, International Code Council, California.

Goel, S.C., Liao, W., Bayat, M.R. and Chao, S.H. (2010), "Performance-based plastic design (PBPD) method for earthquake-resistant structures : An overview", *Struct. Des. Tall Spec. Build.*, **137**(19), 115-137. https://doi.org/10.1002/tal.547.

Hwang, S.J., Fang, W.H., Lee, H.J. and Yu, H.W. (2001), "Analytical model for predicting shear strength of squat walls", *J. Struct. Eng.*, ASCE, **127**(1), 43-50. https://doi.org/10.1061/(ASCE)0733-9445(2001)127:1(43).

IS:1893-I (2016), Criteria for Earthquake Resistant Design of Structures, Bureau of Indian Standards, New Delhi.

Jain, S.K., Lettis, W.R., Murty, C.V.R. and Bardet, J. (2002), "Bhuj, India earthquake of January 26, 2001 reconnaissance report", *Earthq. Spectra*, **18**(S1), 297-317.

Júlio, E.N.B.S. and Branco, F.A.B. (2008), "Reinforced concrete jacketing-interface influence on cyclic loading response", *Am. Concrete Inst. Struct. J.*, **105**(4), 1-7.

Karamodin, A. and Zanganeh, A. (2017). "Seismic design and performance of dual moment and eccentrically braced frame system using PBPD method", *Lat. Am. J. Solid. Struct.*, **14**(3), 441-463. https://doi.org/10.1590/1679-78253425.

Kato, D. and Ohnishi, K. (2001), "Axial load carrying capacity of R/C columns under lateral load reversals", *Proc. Third U.S.-Japan Workshop on Performance-based Earthq. Eng. Meth. for Reinf. Conc. Build. Struct.*, 231-239.

Kumar, P.C.A. and Sahoo, D.R. (2016), "Optimum range of slenderness ratio of hollow steel square braces for special concentrically braced frames", *Adv. Struct. Eng.*, **19**(6), 928-944. https://doi.org/10.1177/1369433216630442.

Kumar, P.C.A., Anand, S. and Sahoo, D.R. (2017), "Modified seismic design of concentrically braced frames considering flexural demand on columns", *Earthq. Eng. Struct. Dyn.*, **46**, 1559-1580. https://doi.org/10.1002/eqe.2867.

Liao, W.C. (2010). "Performance-based plastic design of earthquake resistant reinforced concrete moment frames", Doctoral Thesis, The University of Michigan, USA.

Moehle, J.P. (2000). "State of research on seismic retrofit of concrete building structures in the US", *Proceedings of the US-Japan Symposium and Workshop on Seismic Retrofit of Concrete Structures-State of Research and Practice*, Japan.

Motter, C.J., Abdullah, S.A. and Wallace, J.W. (2018), "Reinforced concrete structural walls without special boundary elements", *ACI Struct. J.*, **115**(3), 723-733.

Murty, C.V.R., Greene, M., Jain, S.K., Prasad, N.P. and Mehta, V.V. (2005), "Earthquake rebuilding in Gujarat, India", Special Earthquake Report, Earthquake Engineering Research Institute, Oakland California.

Nagaprasad, P., Sahoo, D.R. and Rai, D.C. (2009), "Seismic strengthening of RC columns using external steel cage", *Earthq. Eng. Struct. Dyn.*, **38**, 1563-1586. https://doi.org/10.1002/eqe.917.

Newmark, N.M. and Hall, W.J. (1982), *Earthquake Spectra and Design*, Earthquake Engineering Research Institute, Oakland California.

Oinam, R.M. (2017), "Metallic energy dissipation devices for seismic strengthening of reinforced concrete frames with soft-storey", Doctoral Thesis, Indian Institute of Technology Delhi, New Delhi.

Oinam, R.M. and Sahoo, D.R. (2016). "Seismic rehabilitation of damaged reinforced concrete frames using combined metallic yielding passive devices", *Struct. Infrastr. Eng.*, **13**(6), 816-830. https://doi.org/10.1080/15732479.2016.1190766.

Oinam, R.M. and Sahoo, D.R. (2018), "Numerical evaluation of seismic response of soft-story RC frames retrofitted with passive devices", *Build. Earthq. Eng.*, **16**(2), 983-1006. https://doi.org/10.1007/s10518-017-0240-5.

Oinam, R.M. and Sahoo, D.R. (2019). "Using metallic dampers to improve seismic performance of soft-story RC frames: Experimental and numerical study", *J. Perform. Constr. Facil.*, **33**(1), 1-18. https://doi.org/10.1061/(ASCE)CF.1943-5509.0001254.

Paulay, T. and Priestley, M. (1992), *Seismic Design of Reinforced Concrete and Masonry Buildings*, John Wiley & Sons, Inc., New York.

Reza Banihashemi, M., Mirzagoltabar, A.R. and Tavakoli, H.R. (2015), "Development of the performance-based plastic design for steel moment resistant frame", *Int. J. Steel Struct.*, **15**(1), 51-62. https://doi.org/10.1007/s13296-015-3004-6.

Sabelli, R., Mahin, S. and Chang, C. (2003), "Seismic demands on steel braced frame buildings with buckling-restrained braces", *Eng. Struct.*, **25**(5), 655-666. https://doi.org/10.1016/S0141-0296(02)00175-X.

Sahoo, D.R. and Chao, S.H. (2010), "Performance-based plastic design of buckling-restrained braced frames", *Eng. Struct.*, **32**(9), 2950-2958. https://doi.org/10.1016/j.engstruct.2010.05.014.

Sahoo, D.R. and Rai, D.C. (2010), "Seismic strengthening of non-ductile reinforced concrete frames using aluminum shear links as energy-dissipation devices", *Eng. Struct.*, **32**(11), 3548-3557. https://doi.org/10.1016/j.engstruct.2010.07.023.

Saravanan, T.J., Rao, G.V.R., Prakashvel, J., Gopalakrishnan, N., Lakshmanan, N. and Murty, C.V.R. (2017), "Dynamic testing of open ground story structure and in situ evaluation of displacement demand magnifier", *J. Perform. Constr. Facil.*, ASCE, **31**(5), 1-20. https://doi.org/10.1061/(ASCE)CF.1943-5509.0001052.

Smyrou, E. (2015), "FRP versus traditional strengthening on a typical mid-rise Turkish RC building", *Earthq. Struct.*, **9**(5), 1069-1089. http://dx.doi.org/10.12989/eas.2015.9.5.1069.

Srechai, J., Leelataviwat, S., Wongkaew, A. and Lukkunaprasit, P. (2017), "Experimental and analytical evaluation of a low-cost seismic retrofitting method for masonry-infilled non-ductile RC frames", *Earthq. Struct.*, **12**(6), 699-712. https://doi.org/10.12989/eas.2017.12.6.699.

Teran, A. and Ruiz, J. (1992), "Reinforced concrete jacketing of existing structures", *Proceedings of the 10th World Conference Earthq. Eng.*, Balkema, Rotterdam, 5107-5113.

Vandoros, K.G. and Dritsos, S.E. (2008), "Concrete jacket construction detail effectiveness when strengthening RC columns", *Constr. Build. Mater.*, **22**(3), 264-276. https://doi.org/10.1016/j.conbuildmat.2006.08.019.

Wallace, J.W. (1994), "New methodology for seismic design of RC shear walls", *J. Struct. Eng.*, ASCE, **120**(3), 863-884. https://doi.org/10.1061/(ASCE)0733-9445(1994)120:3(863).

Yavari, H., Ghobadi, M.S. and Yakhchalian, M. (2019), "Progressive collapse potential of different types of irregular buildings located in diverse seismic sites", *Heliyon*, **5**(1), e01137. https://doi.org/10.1016/j.heliyon.2019.e01137.

*JK*

## Symbols

| | |
|---|---|
| $A_c$ | Area of concrete column |
| $D_c$ | Compression force in diagonal strut |
| $E_d$ | Dissipated energy |
| $E_i$ | Seismic input energy |
| $E_p$ | Plastic energy |
| $M^r_{pc}$ | Moment demand on column |
| $R_\mu$ | Ductility reduction factor |
| $T$ | Fundamental time period |
| $V_{pc}$ | Shear capacity of column |
| $V_y$ | Design yield base shear |
| $d_m$ | Diagonal length of infill panel |
| $h_m$ | Height of infill panel |
| $t_{inf}$ | Thickness of infill panel |
| $\alpha$ | Dimensionless parameter |
| $\gamma$ | Energy modification factor |
| $\theta$ | Angle masonry strut (radians) |
| $\theta_u$ | Ultimate drift |
| $\lambda_h$ | Dimensionless parameter |
| $\mu_s$ | Structural ductility factor |
| $C_d$ | Displacement amplification factor |
| $E_c$ | Modulus of elasticity of concrete |
| $E_i$ | Input seismic energy |
| $E_m$ | Modulus of elasticity of masonry |
| $F_h$ | Tension forces in the horizontal ties |
| $I_c$ | Moment of inertial of column |
| $L_m$ | Clear span of bay |
| $M_{pc}$ | Moment capacity of column |
| $P$ | Axial force |
| $R_m$ | Diagonal compression force in masonry panel |
| $S_a$ | Spectral acceleration |
| $V$ | Shear force on masonry panel |
| $V^r_{pc}$ | Shear demand on column |
| $W$ | Seismic weight |
| $h$ | Column height between centerlines of beams |
| $n_c$ | Numbers of ground story columns |
| $w$ | Effective width of strut |
| $z_m$ | Length of contact for masonry |
| $\eta$ | Factor to account for pinched hysteretic behavior |
| $\theta_p$ | Plastic rotation capacity of ground column |
| $\theta_y$ | Yield drift |
| $\varphi$ | Curvature |
| $\phi$ | Bar diameter in mm |